CHAPTER 3 METHODOLOGY

3.1 Introduction

The crack development in the rock mass surrounding caverns under the applied internal pressure conditions described in the previous research (Tunsakul et al., 2013) indicated that the stress state prior to applying the internal pressure, has a strong influence. The behavior initiates with the concentration of strains in zones of limited extension. The zones then grow, and at a certain stage, the strain is localized and forms a failure plane. Consequently, this localized fracture propagates from the cavity up to the ground surface for cases of k less than or equal to 1, which can lead to collapse of the cavity roof. This so-called progressive failure is a topic of considerable discussion. Commonly, in mining and other tunneling operations, failure at compressive stress concentrations is of a major concern, and primary tensile fractures are rare because the confining pressure is usually high enough to suppress the tensile stress concentration at the cavity wall. For the problem of caverns under high internal pressure, the numerical investigation based on FEM in conjunction with contact-friction interface treatment by Tunsakul et al. (2013) reveals that, by comparing the numerical results with those from physical model tests, it can be inferred that tensile fracture governs crack propagation in their study. In the analyses, both shear and tensile failure modes were considered. However, the study was limited on only the artificial rock used in the study which is brittle with low strength. With the diverse properties of in-situ natural rock, more extensive investigation should be done covering all range of possible rock properties. Moreover, wider range of stress, particularly under in-situ condition, should be also further considered.

3.2 Concept for evaluation of failure behavior

Many numerical modeling procedures have been developed in rock mechanics for analysis of various types of underground excavations. Numerical method is often used to evaluate the fracture in rock mass. It is well known that full analysis of localization problems requires very heavy computation. A more simple, but adequately acceptable, method is preferred. Note that, to capture the detail of the processes involved in progressive fracturing, sophisticated numerical methods (such as RFPA by Tang (1997) and Zhu et al. (2005)) are necessary. It is known that the analysis results when distributed failure surfaces are localized into one failure surface do not show much difference from those where one failure surface is assumed from the beginning. Therefore, a simplified analysis method by standard finite element method with contact-friction interface treatment (Adachi, et al., 1985; Tunsakul et al., 2013) was adopted in this study. To fulfill the evaluation of the failure path, the analyses are carried out to identify the failure initiation point and propagation. The initiation point is evaluated from the consideration of both shear and tensile failures. Paths of failure surfaces in a rock mass are determined based on the stress field and associated directions of possible failure planes at any location. The analyses in this study are conducted by using the continuum finite element program ABAQUS (ABAQUS, 2010).

To fulfill the evaluation of the failure path, the analyses are carried out to identify the failure initiation point and fracture propagation path. The analysis thus starts with stress analysis of the problem considered under increasing cavern pressure. The initiation point can be evaluated from the stress states obtained together with the consideration of both shear and tensile failures. To evaluate the failure path based on the stress field

obtained, the directions of failure planes at any location were calculated. The failure surface can then be estimated from that starting point by following the calculated failure plane direction vectors at any location.

The steps of the methodology in this study can be illustrated as the flow chart of overall framework as shown in Figure 3.1. The details and necessary features of each step are described in the following sections.

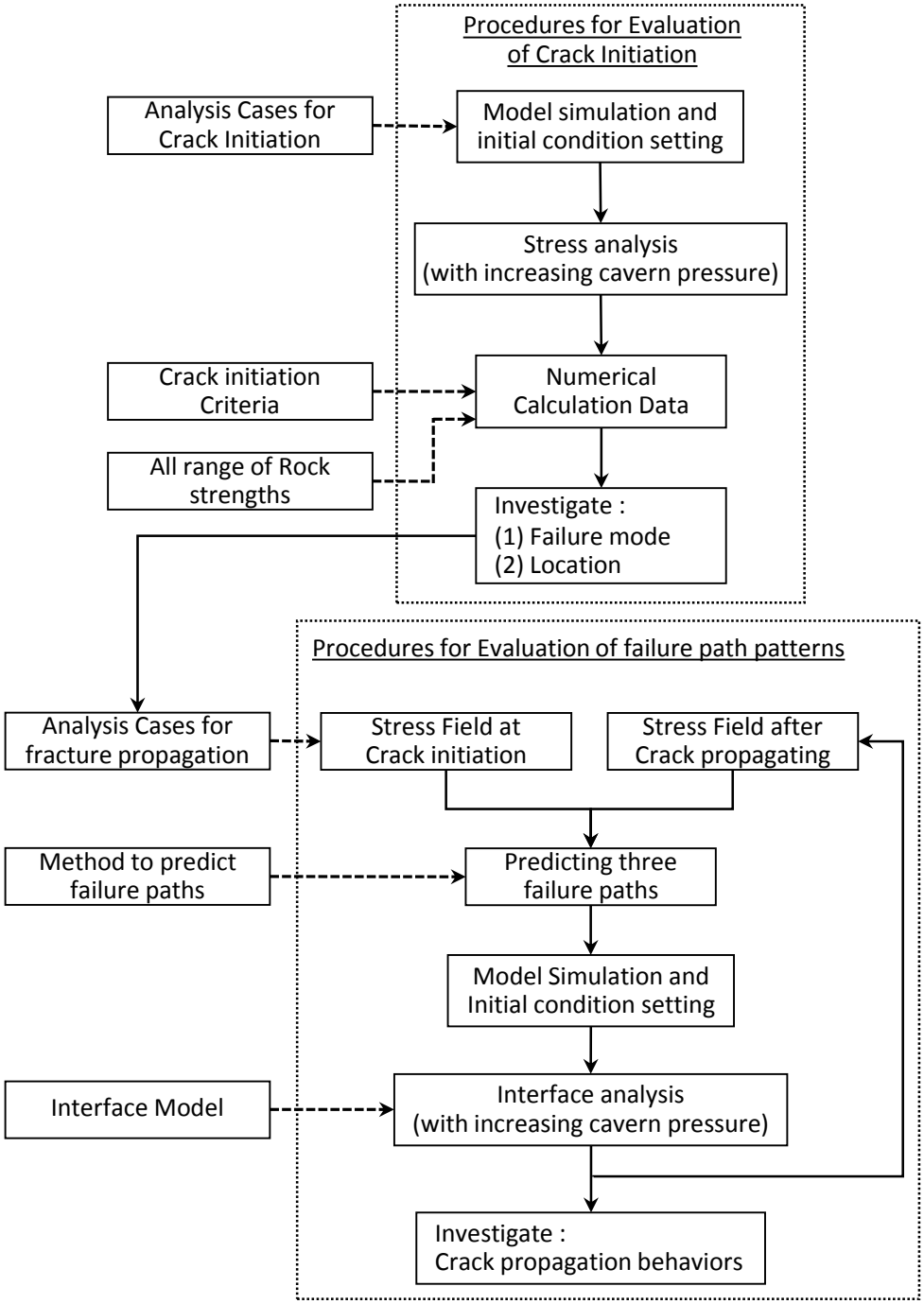

Figure 3.1 Flow chart of overall framework for analysis to evaluate failure path in this study

3.3 Characteristic of problem and rock properties

In this section, the prototype aspects of the cavern and rock properties used in this study are described. The simple silo shape of underground opening is selected to consider. The cavern with an inner diameter of 22.2 m and 33.3 m tall is located at a depth of between 60 – 150 meters as shown in Figure 3.2. This research does not consider some CGES aspects such as shaft tunnel, upper access tunnel, lower access tunnel and a rock reinforcement support.

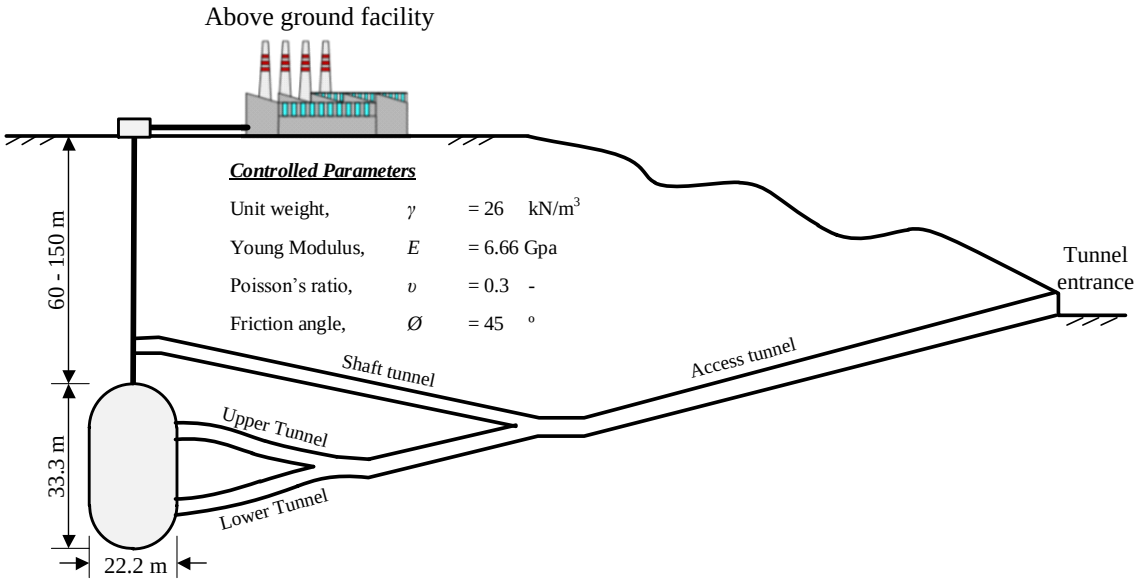

Figure 3.2 Prototype of problems considered in this study (after Johansson, 2003)

In term of parameters used in this study, it can be divided into 2 groups that are controlled rock properties and varying rock properties. The controlled rock properties include unit weight (γ), Young's modulus (E), Poisson's ratio (ν) and internal friction angle ($\emptyset$) as shown in Table 3.1. The rock is assumed to be a linear elastic medium with the set of controlled parameters used as listed in Table 3.1.

Table 3.1 Controlled rock properties

Quantity	Symbol	Value	Unit
Unit weight	γ	26	kN/m^3
Young modulus	E	6.66	GPa
Poisson's ratio	ν	0.2	-
Friction angle	$\emptyset$	45	°

The varying rock properties consist of initial stress ratio (k) and rock strengths. Previous studies reveal that the k has strong influence on failure patterns of tunnels in tunneling work and under high internal pressure (Tunsakul et al., 2013). In this study, the k values in a range between 0.3 – 3.5 are considered. Figure 3.3 shows the range of initial stress ratio (k) found in the natural rock (Hoek and Brown, 1980).

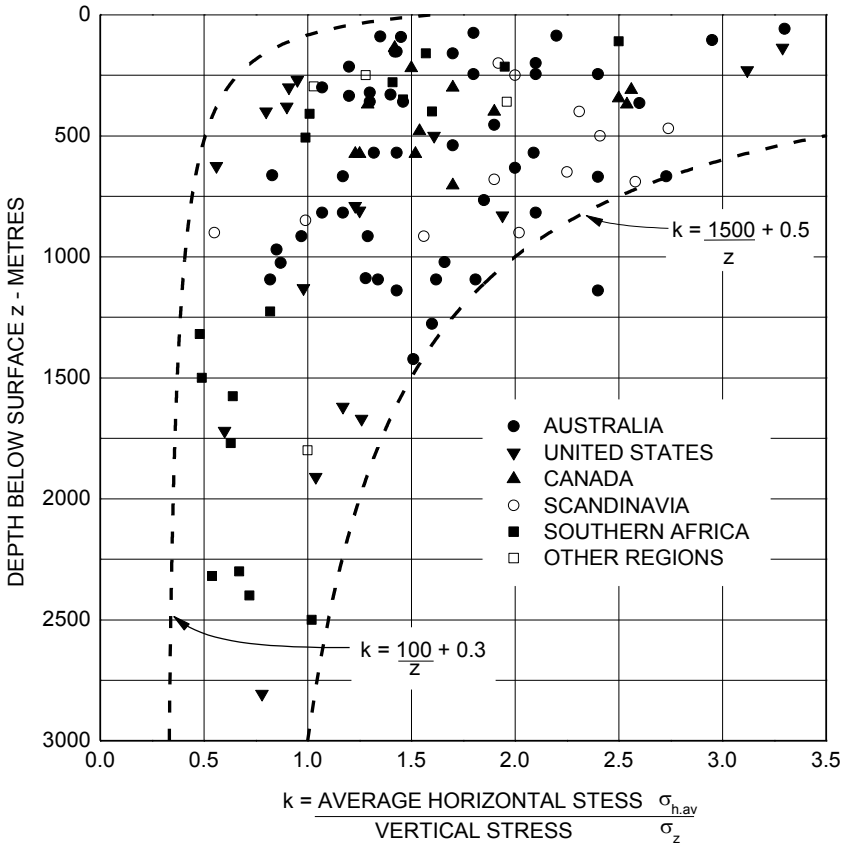

Figure 3.3 Range of initial stress ratio (after Hoek and Brown, 1980)

Based on the idea that the tensile failure criterion of rock mass depends on the tensile strength while the frictional angle and cohesion represent for shear failure criterion, possible ranges of these values of natural rocks should be considered in the analysis. It is found that the frictional angles of natural rocks vary in a narrow range. From previous study, Farmer (1983) presents a range of relationship between tensile strength (σ_t) and cohesion (C) of each rock type as shown in Table 3.2. This information can be rearranged to be the possible natural rock strength boundaries by plotting and making boundaries as shown in Figure 3.4. It is revealed that the minimum and maximum values of tensile strength (σ_t) and cohesion (C) are in range 2 – 35 and 3 – 60 MPa respectively.

Table 3.2 Typical rock strength (Farmer, 1983)

Rock Types	Tensile Strength (MPa)	Cohesion (MPa)
Granite	7-25	14-50
Dolerite	15-35	25-60
Basalt	10-30	20-60
Quartzite	10-30	20-60
Sandstone	4-25	8-40
Shale	2-10	3-30
Limestone	2-25	10-50

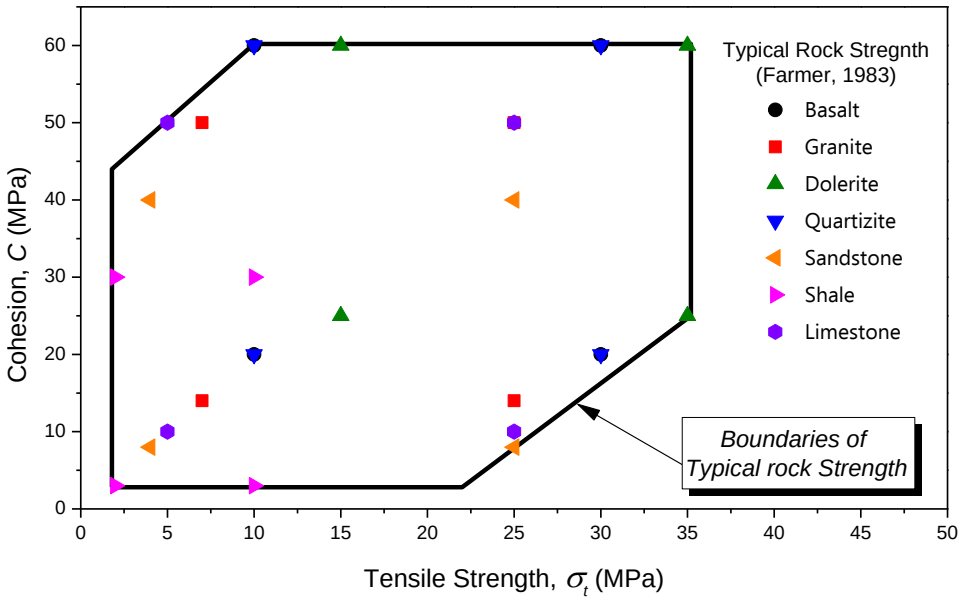

Figure 3.4 Possible natural rock strength boundaries (after Farmer, 1983)

3.4 Concept for evaluation of failure behavior

3.4.1 Analysis Cases for evaluation of crack initiation

The initial stress ratio (k) and depth of cavern are input variables for ABAQUS program, thus, both input variables are varied by incremental as shown in Table 3.3. In term of rock strengths, tensile strength and cohesion, used to evaluate the crack initiation criteria by numerical techniques with the results of stress analysis which are σ_1 and σ_3, will be described below.

Table 3.3 Input parametric variables used for evaluation of crack initiation with ABAQUS

Quantity	Symbol	Value	Unit
Depth	*d*	60, 80, 100, 150	m
In-situ stress ratio	*k*	0.3, 0.6, 0.8, 0.9, 1, 1.2, 1.5 , 3	-

In order to analyze this problem, the 2-D axisymmetric condition is used. Four nodes elements with the controlled aspect ratio in the range of 1-2 are used to model the rock mass. The analytical mesh model and boundary conditions used in this study are shown Figure 3.2. It is noted that the model in Figure 3.2 is only used for evaluating crack initiation and calculating stress field to predict failure paths.

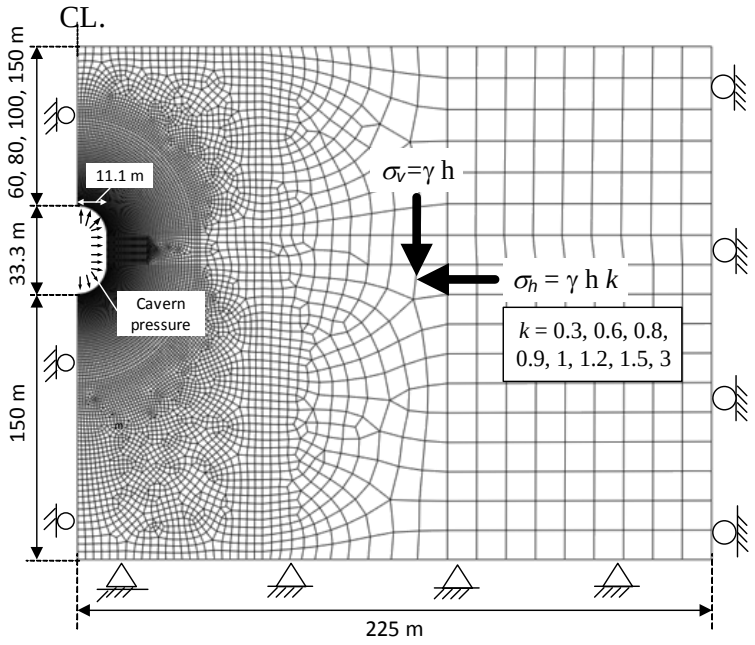

Figure 3.5 Analytical mesh and boundary conditions used in stress analysis

3.4.2 Crack initiation criteria

It is well known that the fracture behavior in this situation (cavern under high internal pressure) has not been well understood yet. The fracture can occur with either shearing or tension mode which might result to different crack patterns. Therefore, both of criteria are used for evaluation of initial crack.

In this section, an approach to find the initiation point of the failure path that occurs due to applying the cavern pressure is described. The point along the cavern surface whose stress state is satisfied when the failure criterion is satisfied is selected as the starting point for failure path. For the tensile mechanism, when the induced tensile stress reaches a critical value, tensile failure occurs. The tensile failure criterion for rock mass is simply written as

$$f(\sigma_1) = \sigma_1 + \sigma_t = 0 \tag{3.1}$$

where ; σ_1 is the major principal stress developed, and σ_t is the tensile strength (tension : negative) of the rock mass.

For shear failure, a number of criteria have been developed for rock (Sheorey, 1997). Among these criteria, the linear Mohr-Coulomb criterion is widely referred to and used in practice because of its simple form and general fit to brittle materials for a range of stresses. The general evaluation of stability of structure is shown in safety factor media. For this section, the evaluation of safety factor is adopted in situation whereas it is used to identify the location of primary crack (not to evaluation of stability of structure). The relationship between current stress state represented by a Mohr circle and the Mohr-Coulomb failure, as graphically illustrated in Figure 3.6, is used to evaluate shear failure in this study. The shear failure is satisfied with τ_s/τ of 1. This ratio is mathematically defined as

$$\frac{\tau_s}{\tau} = \frac{D}{R} = \frac{2C\cos\phi + (\sigma_1 + \sigma_3)\sin\phi}{\sigma_1 - \sigma_3} \tag{3.2}$$

where ; C and ϕ are cohesion and friction angle of rock mass. The parameters σ_1 and σ_3 stand for major and minor principal stresses, respectively.

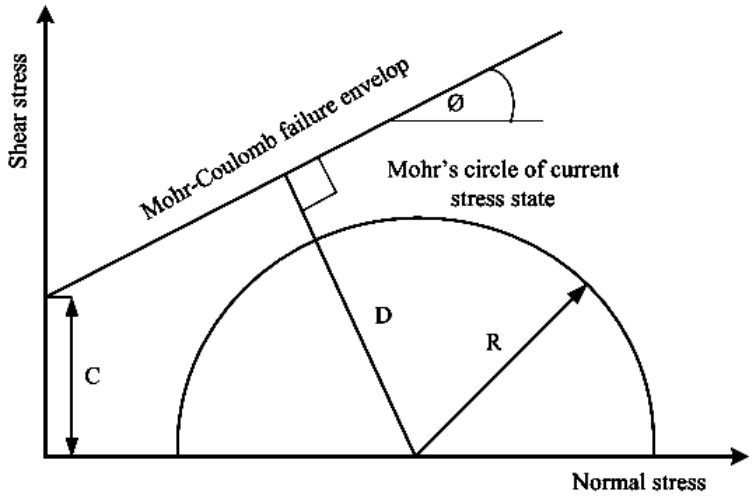

Figure 3.6 Graphical illustration of shear failure criterion, referring to a Mohr circle with its Mohr-Coulomb failure criterion (Tunsakul et al., 2013)

3.4.3 Procedures for evaluation of crack initiation

As previously described in section 3.2, there are two main parts for evaluation, i.e. crack initiation and propagation. In the part of crack initiation evaluation, the details for

procedures can be schematically illustrated as shown in Figure 3.7. The main procedures are specifying the analysis cases; stress analysis to obtain the stress field; failure initiation evaluation and then obtaining the results in terms of failure mode and location. In the evaluation, all possible values of rock strengths are considered

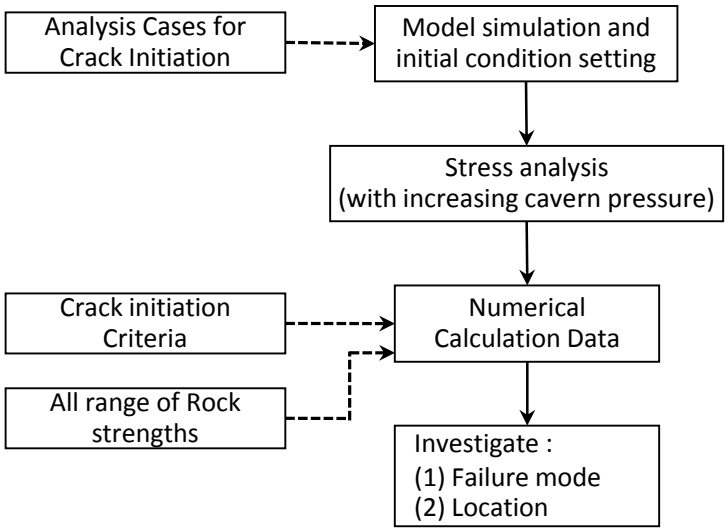

Figure 3.7 The procedure for evaluation of crack initiation

The study thus started with series of stress analyses covering all considered conditions. In order to obtained the reasonable stress field, actual stages of loading must be modeled in the analysis. These include in-situ stress generation, excavation and application of internal stress step-by-step. Figure 3.8 shows the initial stress ratio setting for the example case with depth of 60 m and k of 1. The contour of σ_{xx} and σ_{xx} at stage of in-situ are shown in the left and right side of this picture. It is seen that $\sigma_{xx} = \sigma_{yy}$ at any locations because k was set of 1. Then the simulation of excavation stage is simply performed by removing the excavated element as shown in Figure 3.9. The excavation state results to the deformation of the rock around the cavern by effect of initial stress ratio (k). It is noted that this Figure is for the example case of depth 60 m and k of 1.

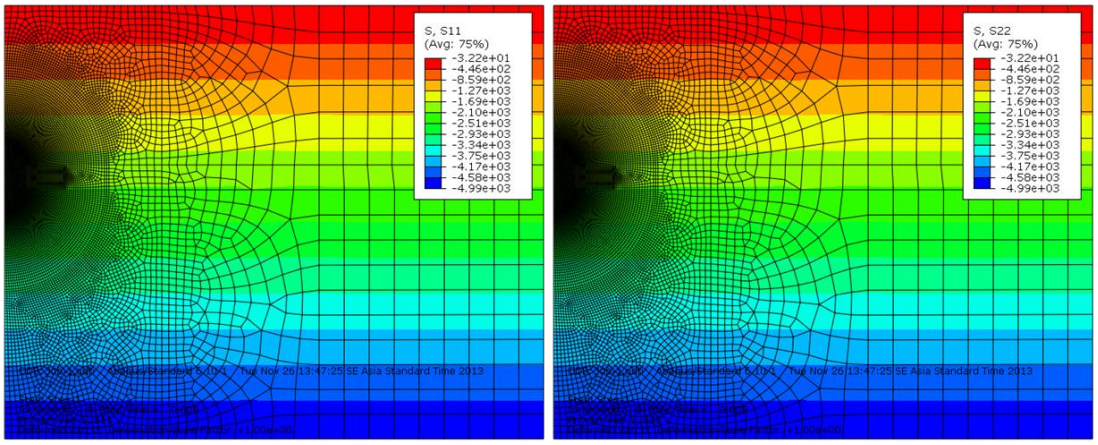

Figure 3.8 Initial stress ratio setting (case of depth 60 m and k of 1)

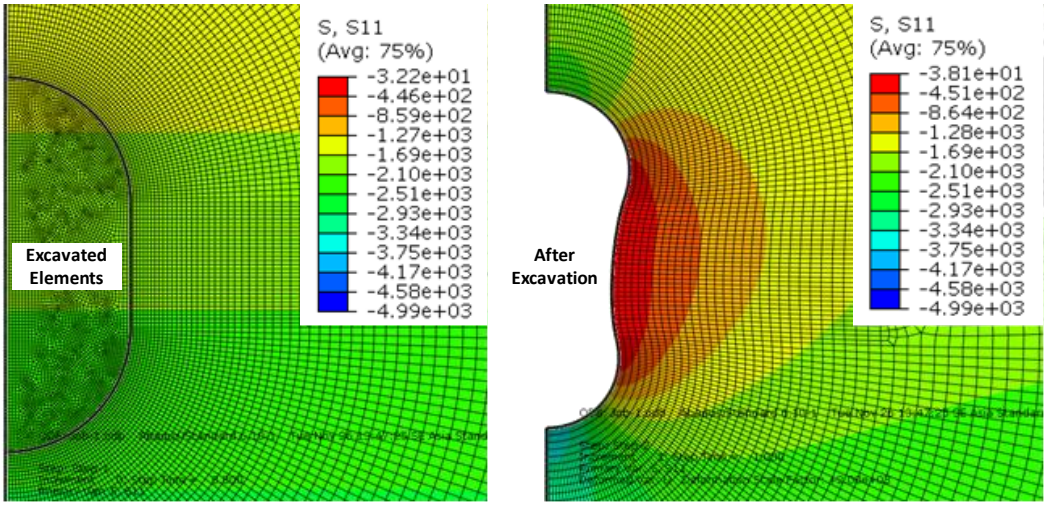

Figure 3.9 Simulation of excavation stage and associated vertical stress distribution

After applying the in-situ stresses, boundary conditions and excavation stage, the cavern pressure gradually increases by applying the stresses on excavated cavern surface from 0 – 100 MPa with 5 MPa increments.

With the stress state obtained during each step, together with the implementation of failure criterion into the program, the evaluation of failure initiation can be done. For tensile failure, the evaluation can be directly done by investigating the evolution of major principal stress (tension: positive). For shear failure evaluation, the D/R concept as described in previous section is numerically implemented via user-subroutine. Figure 3.10 shows the contour of σ_1 and *D/R* with its maximum and minimum value respectively at the same level of cavern pressure for the example case. The values of max σ_1 and min *D/R* are used to evaluate if the tensile or shear failure initiates.

In addition, both output variables of all analysis cases with increasing of the cavern pressure are collected in the calculation data in order to summarize the analysis results and evaluate the crack initiation behaviors. The overall results of this analysis part will be described in section 4.2.

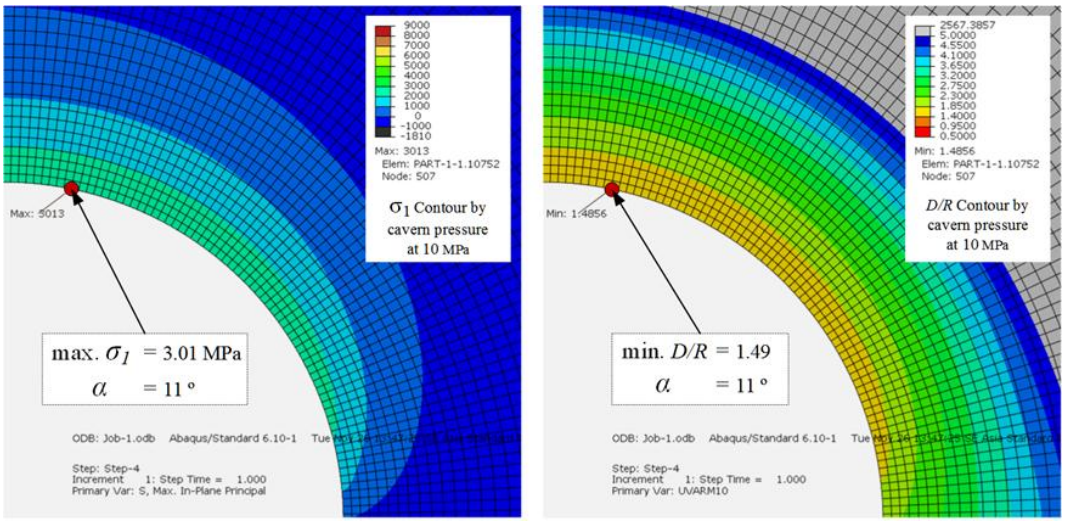

Figure 3.10 Example of the observation of stress state

3.5 Evaluation of fracture propagation behaviors

In this section, method for evaluation of fracture propagation behaviors are described which is performed by FEM with interface contact interaction. There are 2 main issues to be explained. These include the details of contact-friction interface treatment and the method to predict the failure paths.

In addition, with considering the wide range of the possible rock properties, the analyzed cases will be specified after the initial crack behaviors were completely concluded. The parameters used in evaluation of fracture propagation will be explained in section 4.3.2

3.5.1 Method to predict failure paths

A method for predicting failure paths is presented in this section. A failure path is predicted by connecting the direction of failure plane at any locations which, in turn, is calculated from the stress state. From the failure modes considered (Tensile and Shear) in this study, there are three possible failure planes. Figure 3.11 shows these three possible failure planes, one is dominated by tensile failure mode. Tensile failure plane is represented by the minor principal plane (plane of σ_1). The remaining two planes are shear failure planes which are in accordance with Mohr-Coulomb Failure as shown in the Figure.

Noted that, commonly, the normal stresses (σ_1, σ_2 and σ_n) and shear stress (τ_{xy}) are employed in the analysis. Since they are vector quantities, therefore, not only the magnitude but also sign conventions must be also considered in the analysis. The sign conventions used in this study are referred to as following, tension is positive (+) and compression is negative (-) for normal stress. The counterclockwise is negative (-) and clockwise is positive (+) for shear stress.

Since the principal stresses are necessary in the calculation, the stresses in Cartesian coordinate must be transformed as illustrated in Figure 3.11. Consequently, the calculated failure plane orientation with respect to the principal planes must be also reconsidered to refer with the Cartesian coordinate.

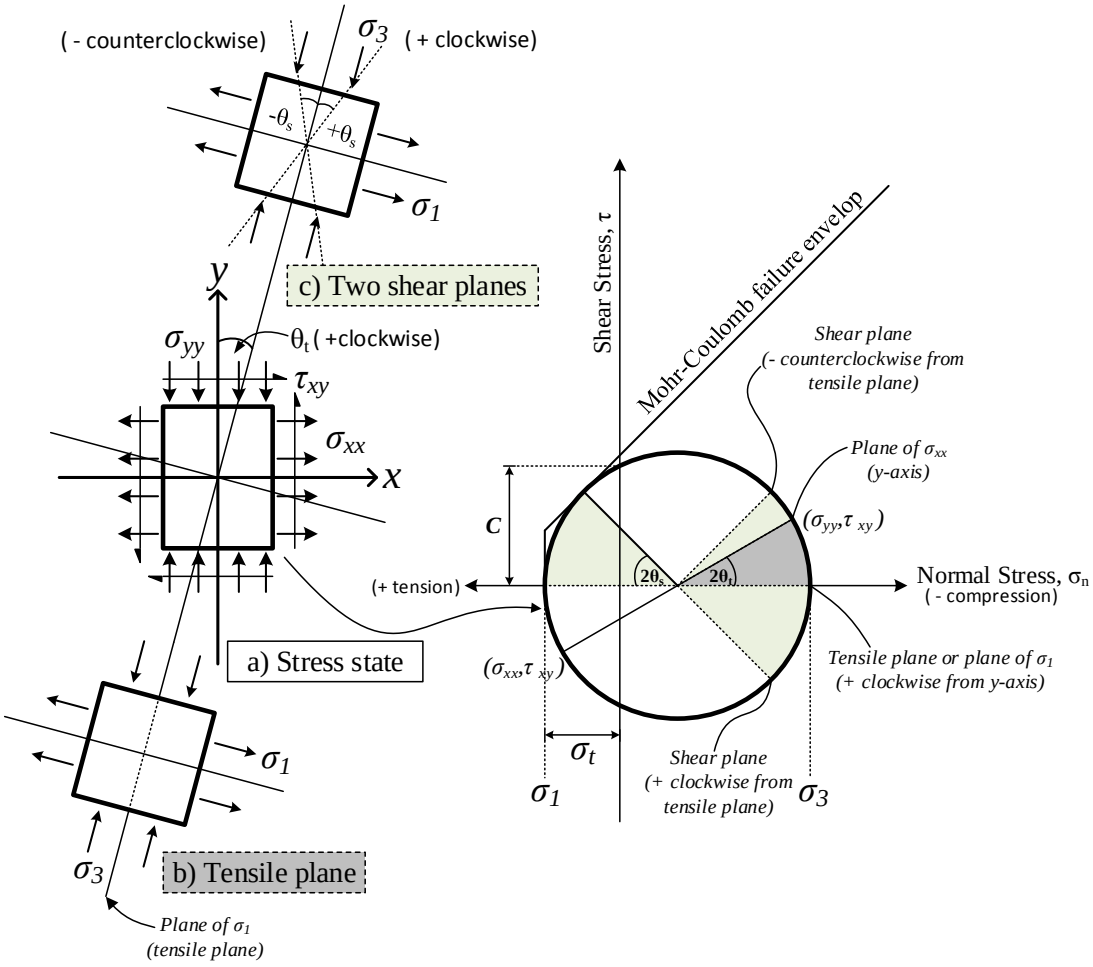

Figure 3.11 Possible failure planes

$$\theta_{t\rightarrow y-axis} = \theta_t = \frac{1}{2}\arctan\left|\frac{2\tau_{xy}}{(\sigma_{xx} - \sigma_{yy})}\right| \tag{3.3}$$

$$\theta_{s\rightarrow y-asix} = \theta_t \pm \theta_s \quad ; \; \theta_s = \left(\frac{90-\phi}{2}\right) \tag{3.4}$$

The method to obtain failure paths can be divided into 2 steps. First step, calculate the failure planes (in angle) from stress component (σ_1, σ_3 σ_{xx}, σ_{yy}, τ_{xy}) of which the stress state reaches crack initiation criterion. Tensile and shear failure planes are calculated by equations 3.3 and 3.4 respectively. Figure 3.7 a) illustrates an example of the possible failure planes at any locations under tensile mode calculated by equation 3.3. On the other hand, two possible shear failure planes calculated by equation 3.4 are shown in Figure 3.7 b)

Second step, after three directions of possible failure planes are calculated and the crack initiation point is specified, by connecting the direction of each failure plane at any locations, the failure paths are obtained.

A method to connect the direction of failure plane is to connect by increment of failure path distance. This increment is adjusted by a distance between two integration points of each element and it should be smaller than that distance. By adding the increment of failure path distance step by step, the possible failure paths are obtained.

A tip of failure path from previous step is used to search for an integration point which is closest. The orientation of the possible failure plane of that integration point is then used to evaluate for the next increment.

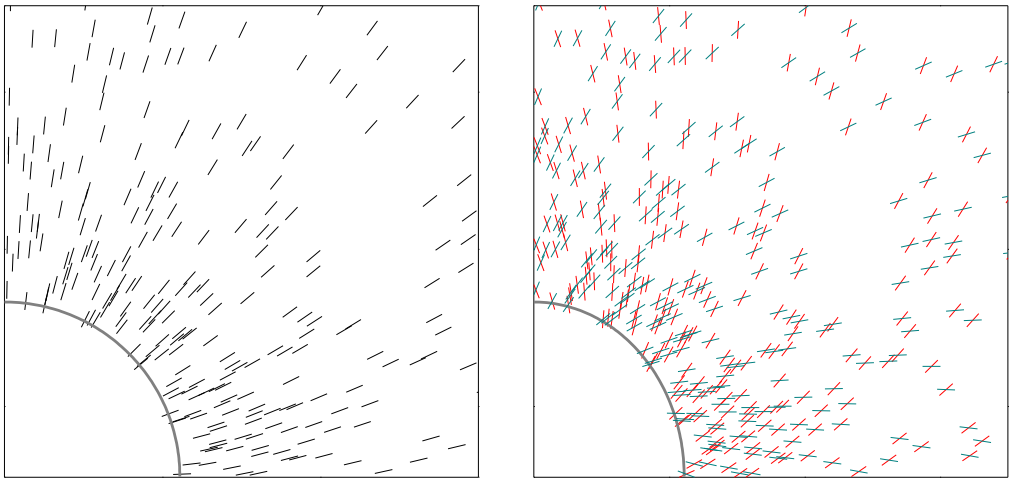

a) Tensile planes b) Shear planes

Figure 3.12 Examples of failure plane calculation

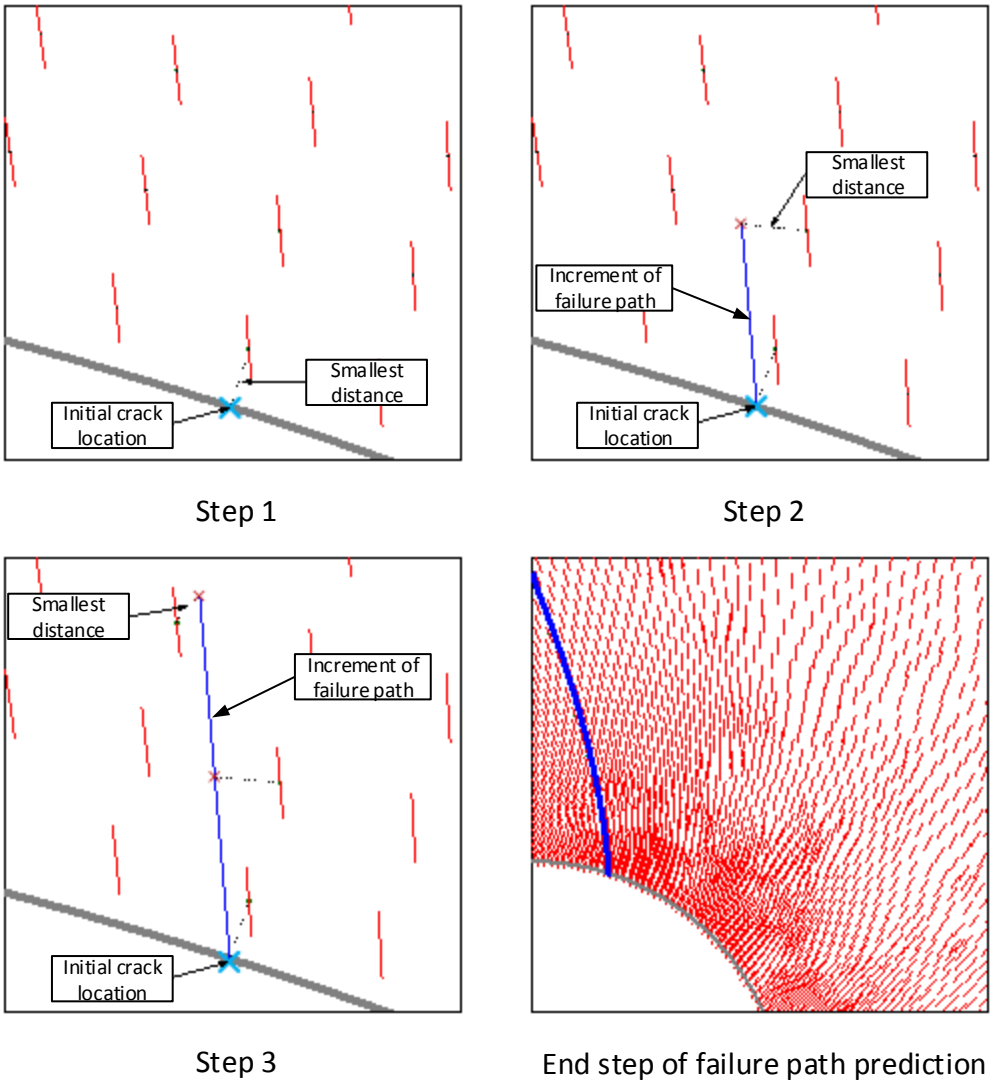

Figure 3.13 Example of method for connecting failure plane

3.5.2 Interface model for progressive failure analysis

The detail of the interface model is explained in this section. The slip or opening of contacts can occur once either shear or tensile failure criterion is satisfied, respectively. Figure 3.14 illustrates the algorithm for the interface contact behavior, as modeled in this study.

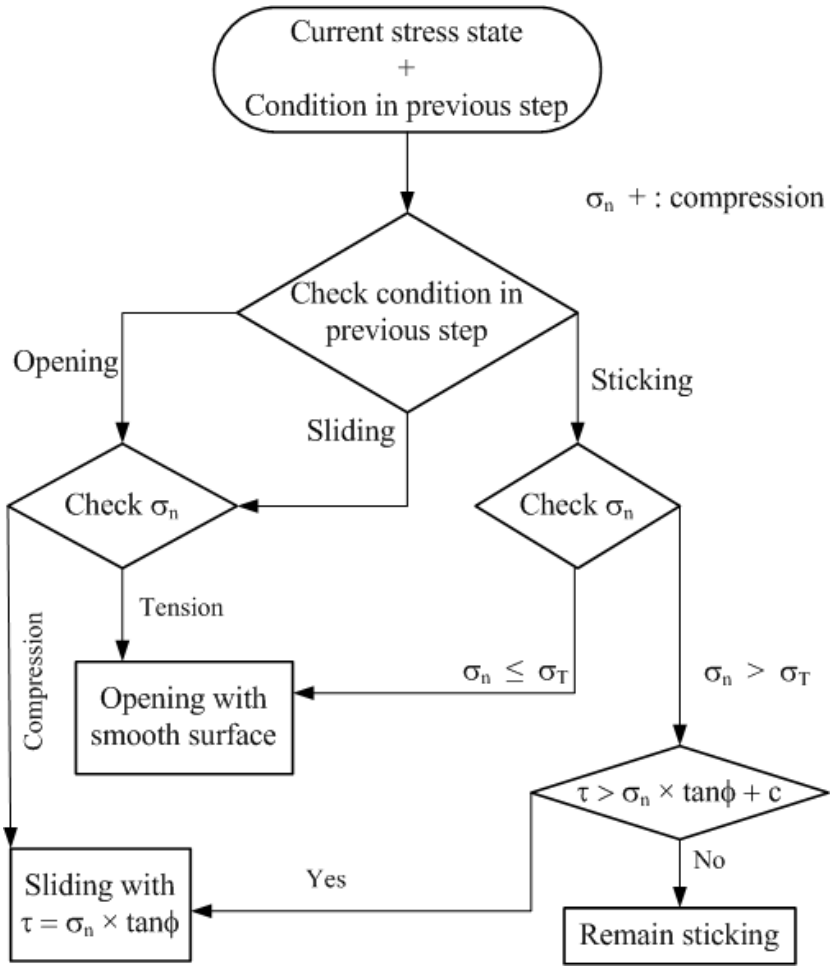

Figure 3.14 Illustrates the algorithm for the interface contact behavior (Tunsakul et al., 2013)

In this study, the dilatancy of the interface is not considered and it is assumed that the shear failure occurs when the shear stress along the predicted failure surface exceeds the Mohr-Coulomb shear strength as written in equation 3.5 and 3.6.

$$\tau > C + \sigma_n \times \tan\phi \tag{3.5}$$

Once the stress state reaches the failure criterion, slip begins and the cohesion becomes zero. The post-failure behavior of the interface is then assumed to follow Coulomb's law:

$$\tau = \sigma_n \times \tan\phi_r \tag{3.6}$$

where $\varnothing_r$ is the residual frictional angle

A special attention is paid to the interface of rock mass along failure path as displacement discontinuity, namely sliding, under certain stress conditions. The interfaces between rock masses follow an elastic-plastic stress-displacement relation. The condition for a relative slip along an interface is governed by a Coulomb law. If the tensile strength of the contact is overcome, the surface separates, creating a gap between them. The finite element program used in this study, ABAQUS, provides an interaction

which is possible to model both normal and friction behaviors separately. The schematic element of interface interaction is illustrated in Figure 3.15.

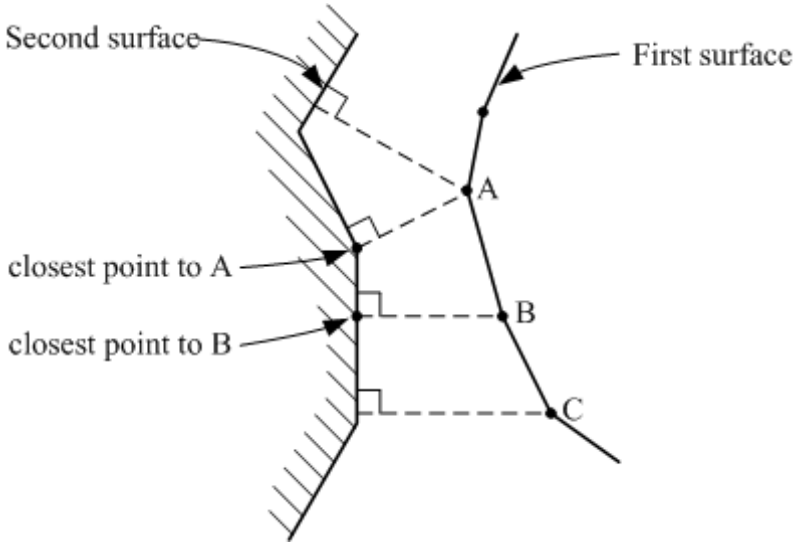

Figure 3.15 Contact and interaction discretization model (ABAQUS Analysis User's Manual, 2010)

3.5.3 Reanalysis for stress redistribution with remeshing technique

In the concept for evaluation of failure behavior by using FEM that was described in section 3.2. The method for identificating the failure initiation point was explained in section 3.4. To accomplish the goals in this study, method to identify fracture propagation path is to more explain in this section.

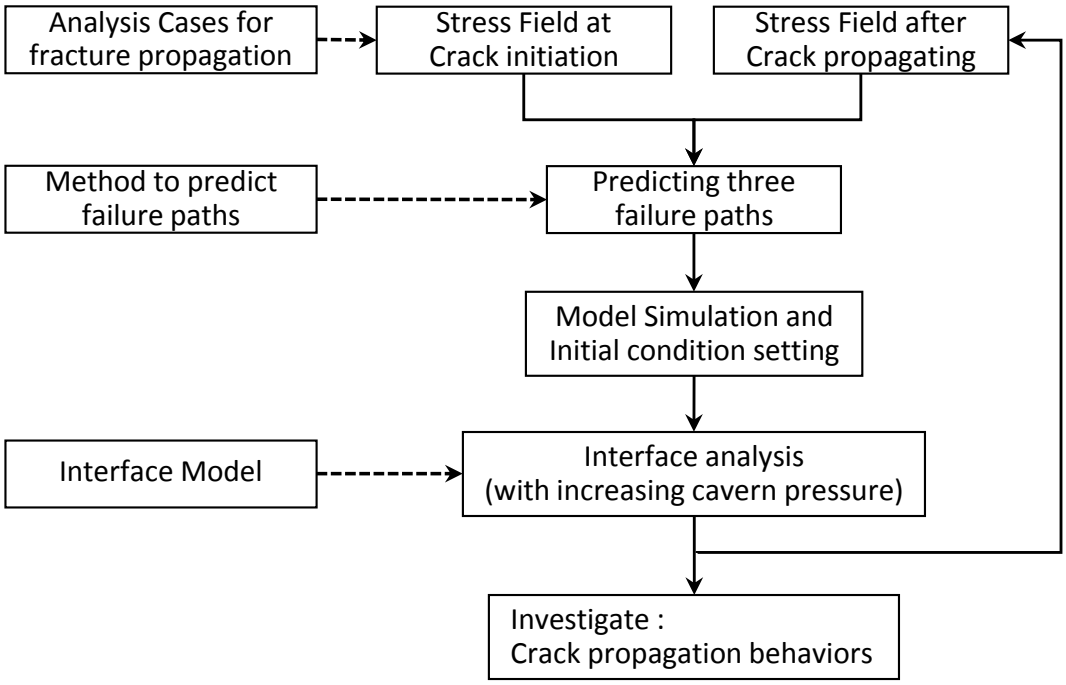

Figure 3.16 The procedure for evaluation of fracture propagation

As the schematic of the procedure for evaluation of fracture propagation shown in Figure 4.10, after crack initiation is specified, the stress states at any locations in the problem at the level of internal pressure to induce crack initiation, are used to predict those three possible failure paths with the method described in section 3.5.2. The failure paths obtained from the stress states at initiating-crack might not be correct because it is based on a certain stress state without consideration of the associated stress redistribution after fracture propagation. Thus, to obtain more accurate results, subsequent analyses of the underground cavern under applied internal pressure are carried out step by step considering partial failure and the stress redistribution is evaluated in each step to update the orientation of the failure planes.

It is noted that the objectives of progressive failure analysis are to evaluate fracture propagation behaviors and orientation of failure patterns. This study performs both possible failure mechanisms concurrently. Therefore, there are three possible failure paths which are needed to be modeled and provided in each step of progressive failure analysis.

Figure 3.17 shows the modeling example of the possible failure paths which are obtained from stress state at crack initiation stress state. Three pre-determined failure paths are then prepared in the new FE mesh as shown in the Figure. Along the prepared possible failure paths, two opposite sides of the region (which are divided by the failure paths) are connected with the contact-interface interaction with the behaviors specified in section 3.6. This model is used to investigate whether which path the crack would propagate. With reanalysis with increasing of cavern pressure, crack propagation along one of the prepared failure path can be seen. For this example, it is observed that the crack propagates along path 2 (path from tensile failure evaluation). With a certain level of applied internal pressure, the crack would propagate for only a certain distance, and a new crack tip would be obtained. By investigating the stress states at this step, the orientations of possible failure paths starting from this new crack tip can be evaluate using the aforementioned procedures. By those repeated procedure, the new mesh for the next step of analysis can be prepared as shown in Figure 3.18. It is noted that three possible failure paths are still prepared, but start from the new crack tip. By repeating the analysis processed incrementally, progressive failure of the rock mass can be done and the failure path is obtained.

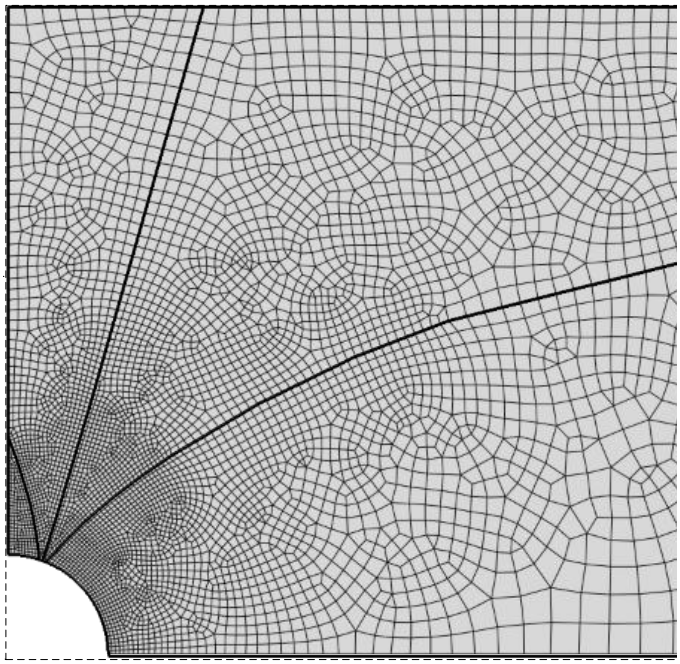

Figure 3.17 FE mesh for three pre-determined possible failure paths starting from crack initiation point

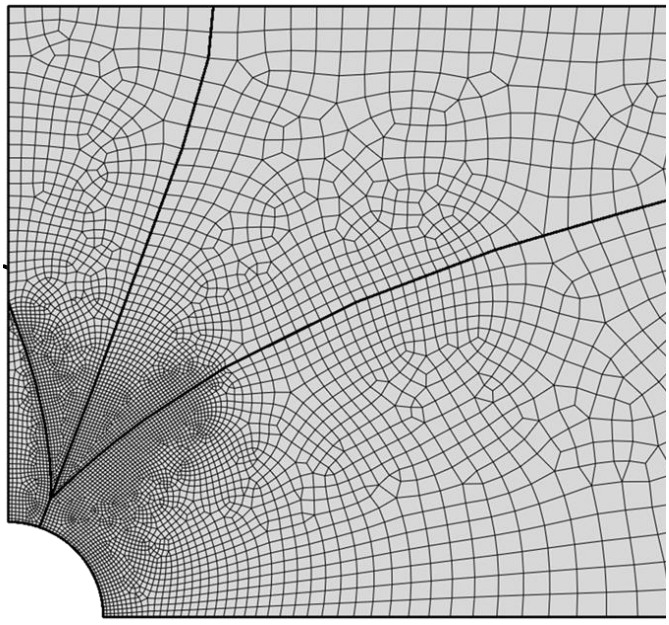

Figure 3.18 FE mesh for three pre-determined possible failure paths starting from the new crack tip

However, such that the analysis cases have to be selected after the crack initiation was summarized and as described of procedure for evaluation of fracture propagation in this section are also not complete yet. In addition, it is due to the fracture propagation analysis which is discretization problem that performed by FEM, have more details to be judged by researcher for each analysis cases, for those reasons, the procedure coincided with the analysis results will be illustrated in next the chapter (section 4.4).